JOURNAL OF GEOPHYSICAL RESEARCH, VOL. 94, NO. B1, PAGES 574-586, JANUARY 10, 1989

TILT OBSERVATIONS USING BOREHOLE TILTMETERS
1. ANALYSIS OF TIDAL AND SECULAR TILT

Judah Levine, Charles Meertens,[1] and Robert Busby[2]

Joint Institute for Laboratory Astrophysics,
National Bureau of Standards and University of Colorado, Boulder

Abstract. We have designed a borehole tiltmeter using two horizontal pendulums which have periods of 1 s. We have installed the instruments at seven sites in Colorado and Wyoming to evaluate the secular tilt, the tides, and the coherence between nearby instruments. Using 28 days of data from Boulder, Colorado, the standard deviations of the tidal estimates are 5% for the semidiurnal component M_2 and 9% for the diurnal component O_1. The estimates agree with models that include the body tide, the ocean load, and the topographic correction to better than the estimated uncertainty. Tidal measurements at Erie, Colorado, have larger, possibly nonrandom variability that may be caused by a coupling between the tides and long-period tilts. The coherence between nearby instruments is $\gtrsim 0.5$ for frequencies ranging from 0.5 to 2 cycles per day, but drops to a much smaller value outside of this range. The secular tilt rate is quite variable and ranges from 0.1 to 1 μrad/yr. Measurements at Erie, Colorado, and in Yellowstone National Park, Wyoming, exhibit an annual or biannual periodicity with an amplitude of about 1 μrad, which is consistent with a $1/f^2$ extrapolation of the diurnal noise power to longer periods.

Introduction

Measurements of tilt tides provide information on the elastic constants of the Earth. Tilt measurements can also be used to study strains in areas of seismic activity and might conceivably be useful as a method of predicting earthquakes.

In order to make unambiguous tilt measurements, the sensor must be both sensitive and stable and as insensitive as possible to environmental perturbations. Furthermore, the instruments must be adequately coupled to the surrounding material so that the recorded tilts are representative of the regional tilt vector.

One method for evaluating the success of a given design is to compare the tilt records obtained from several closely spaced independent instruments. Except at tidal periods, previous comparisons of this type have not been very successful, especially for instruments installed in shallow boreholes [Wyatt and Berger, 1980; Wyatt et al., 1982]. The lack of coherence has been ascribed to short-wavelength tilts, perhaps produced by thermoelastic stresses or to a residual sensitivity of the instrument to various extraneous effects such as temperature, air pressure, or variations in the water table.

Efforts to improve the performance of tiltmeters can be divided into two broad categories: increasing the length of the baseline to average or dilute the very local effects, and installing the instrument in a deeper hole to improve the isolation between the instrument and the spurious effects that are presumed to be larger near the surface. We have chosen the latter method: to try to improve tilt metrology by installing small sensors in relatively deep boreholes.

If the goal is to measure tectonic tilts accurately, then our degree of improvement would be measured by a decreasing sensitivity to known events such as heavy rainstorms or by a decrease in rate (or increase in smoothness) of the observed secular tilt. Indeed, we find that deeper instruments are better in these senses. Figure 1 compares the response of instruments at different depth to rainfall. The secular tilt recorded by the deeper (but otherwise very similar) instrument is unaffected by several heavy rainstorms and is smoother overall.

The performance of an instrument at tidal frequencies is a useful indicator of its potential for long-period measurements. In addition, the response at tidal periods is often useful in itself. Even if the amplitude and phase of the tidal admittance are not known at a particular site, a tidal analysis can be used to study the stability of the instrumental gain, the linearity of the sensor, and the sensitivity of the system to extraneous effects.

A measurement of the Earth tides can also be used to study spatial or temporal variations in the elastic properties of the material near the surface. Beaumont and Berger [1974] predicted a spatial dependence in the amplitude and phase of the Earth tides near the boundary between regions of different seismic velocity. They estimated that a contrast of 10% in V_p might produce a change of up to 40% in the amplitude of the tides. This effect would be largest near the velocity discontinuity and would be of comparable magnitude for either tilt or strain observations. The effect on gravity tides would be much smaller and would probably not be observable with existing instrumentation.

Measurements of strain or tilt tides near a fault zone might also be affected by the discontinuity in elastic properties near the fault. Measurements near the Hunsrück fault zone, for example, show that the magnitude of M_2 changes by up to 70% along an east-west azimuth, while the north-south amplitude shows an even greater variation [Bonatz et al., 1983; Gerstenecker et al., 1985].

[1]Now at Department of Geology and Geophysics, University of Utah, Salt Lake City.

[2]Now at Lamont-Doherty Geological Observatory, Palisades, New York.

Paper number 88JB03598.
0148-0227/89/88JB-03598$05.00

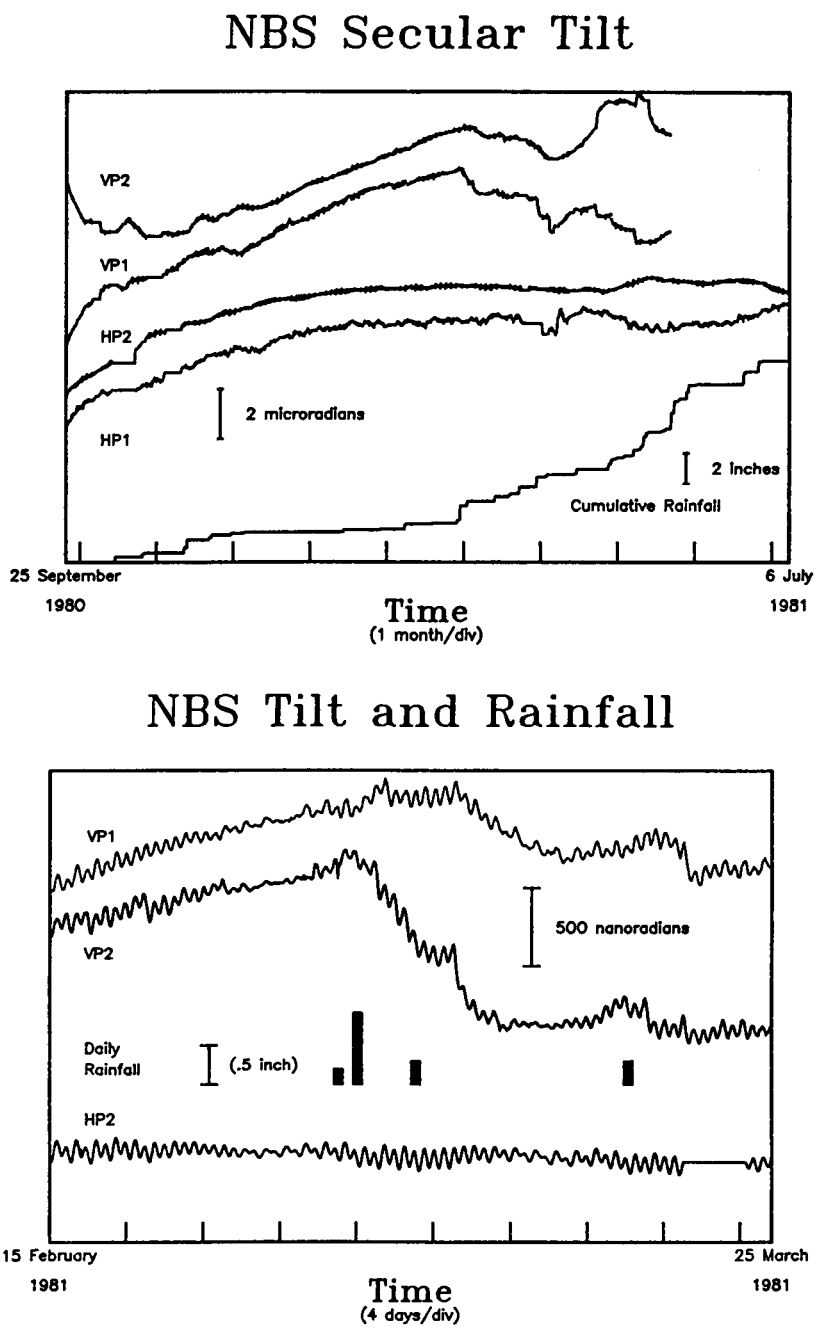

Fig. 1. Tiltmeter VP is a pair of vertical pendulums in a 15-m borehole, and tiltmeter HP is a pair of horizontal pendulums in a 30-m borehole. The response of the instruments to rainfall is shown. (a) Data record approximately 10 months long. (b) Shorter segment of the record to show the effect of rainfall more clearly.

In this paper we report on the design of a borehole tiltmeter and on the methods that we have developed for recording and analyzing tilt data. In a companion paper [Meertens et al., this issue], we will apply our method to a study of Yellowstone National Park in Wyoming. Although our instrument will respond to a wide spectrum of tilts, most of our efforts have been concentrated on the tidal portion of the spectrum. Signals at both longer and shorter periods are more likely to be contaminated by thermal effects and by changes in the level of the water table.

Borehole Design

The boreholes are nominally 15 cm in diameter and 30 m deep. We have experimented with boreholes of different depths, but almost all of the data presented here were recorded by instruments installed at this depth. The holes are drilled using conventional water well drilling equipment. The bottom portion of the hole must be vertical to within 5°. A carbon steel casing, 135 mm in diameter with 6-mm walls, is pressed into the hole. The casing is welded into a continuous, water-tight pipe as it is inserted. The casing

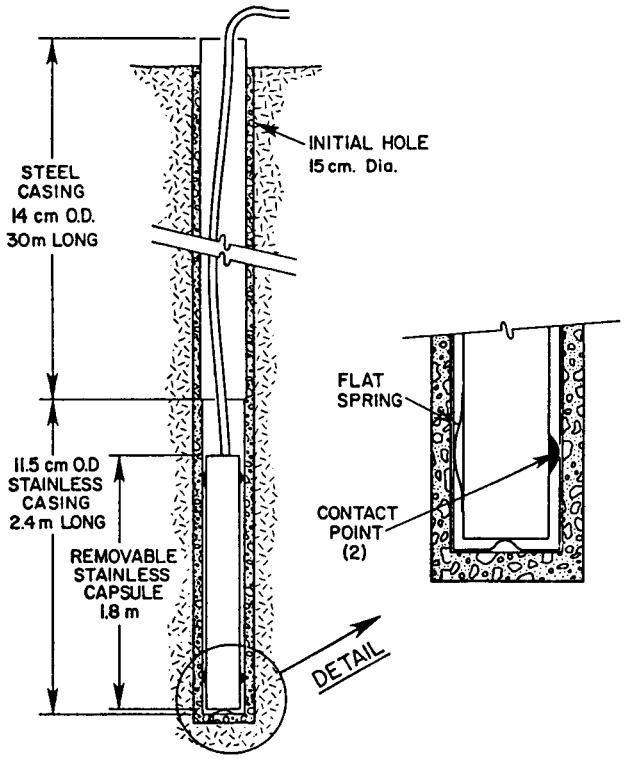

Fig. 2. Schematic diagram of the tiltmeter capsule inserted into the cased borehole. All dimensions are nominal, and the figure is not to scale.

terminates at the bottom in a stainless steel section used to hold the tiltmeter capsule. The bottom section is 2.4 m long and 115 mm in outside diameter. It is sealed by a plate welded across the bottom. A hemispherical knob is welded to the inside of the bottom plate to support the weight of the tiltmeter capsule.

The casing is sealed in place by means of cement poured down to the bottom of the hole before the casing is inserted and around the sides of the casing after it is in place. Some sites have a second, larger diameter casing that is used to keep the top portion of the borehole from collapsing after the drill is removed and before the primary casing can be installed. The larger casing is 210 mm in diameter. The casing extends about 1 m above the surface and is sealed by a removable steel cap.

Instrument Capsule

The instrument capsule is a 1.8-m length of stainless steel tubing closed at the bottom and having a pair of contact points and a flat spring welded on near its top and a second pair with a second flat spring near its bottom. The top of the capsule is sealed with a cap attached by screws and containing an O ring.

The capsule was designed to minimize tilt-strain coupling due to cavity effects. Harrison [1976] showed that there is no cavity effect if the side of the borehole is used as a reference axis for the tiltmeter and only a small effect if the center of the bottom is used as another reference point.

The cables connecting the capsule with the surface are left slack; their weight is supported by a bracket fastened to the top of the casing. See Figure 2.

Capsule Orientation

The capsule is usually not visible from the surface, and its orientation cannot be determined by direct sighting. We use a system of light rods instead. A post is welded to the top cap of the tiltmeter with a flat side aligned with the axis of one of the sensors. A rod can be fastened to the post and is held in place by means of a trapped ball. As the capsule is lowered, additional sections of rod are added. Each section is notched and can only be attached in one orientation using a small screw. After the orientation of the topmost notch is determined using a compass and a transit, the entire series of rods is removed from the capsule by pulling upward, thereby disconnecting the bottom rod from the post.

This method can be used to determine the azimuth of the sensors to within a few degrees. An uncertainty of only 1° is possible if great care is used and under very favorable conditions.

Once the tilt admittance has been determined along two orthogonal azimuths at any site, the orientation of any other instrument may be determined from the tidal data alone. This is most easily done using M_2, which is usually the largest component in the spectrum. If the amplitude and phase of the tilt along azimuth θ_1 are A_1 and ϕ_1, respectively, and if the corresponding values along azimuth θ_2 ($=\theta_1 + 90°$) are A_2 and ϕ_2, then the amplitude and phase that would be observed along some other azimuth α are given by

$$A(\alpha) = \left\{ A_1^2\cos^2(\alpha-\theta_1) + A_2^2\sin^2(\alpha-\theta_1) - A_1A_2\sin 2(\alpha-\theta_1)\cos(\phi_1-\phi_2) \right\}^{1/2} \quad (1)$$

$$\phi(\alpha) = \tan^{-1} \times \left\{ \frac{A_1\sin(\phi_1)\cos(\alpha-\theta_1) - A_2\sin(\phi_2)\sin(\alpha-\theta_1)}{A_1\cos(\phi_1)\cos(\alpha-\theta_1) - A_2\cos(\phi_2)\sin(\alpha-\theta_1)} \right\} \quad (2)$$

where the azimuths are measured clockwise from north, the amplitudes are measured in nanoradians (or other convenient units), and the phases are measured with respect to a common phase origin such as the phase of the local tidal potential at some convenient epoch.

These equations are often used to compute the tilt along any azimuth from the theoretical tilt along two coordinate directions such as north-south and east-west, but they are independent of the tidal theory and depend only on the vector nature of tilt and on the fact that the signals recorded by all of the instruments are derived from a common effective tilt vector at the site (as opposed to a local effect within a single borehole or a spurious instrumental effect). As such, they allow the azimuth of any tiltmeter to be determined. Since our tiltmeters consist of two independent orthogonal sensors, the instru-

ment simultaneously measures the tidal admittance along azimuths α_1 and $\alpha_1 + 90°$. The measured phase difference between the two sensors and the measured amplitude ratio provide two independent estimates of the azimuth: the first using two applications of (2) and the second using two applications of (1). The estimate based on the phase difference is independent of the calibration factors of the pendulums and therefore provides a very robust estimate of the azimuth limited only by the uncertainty in the admittance estimate. The amplitude ratio provides a second determination of the azimuth if the calibration factors are known to be constant; otherwise it serves as a continuous check on the ratio of the calibration factors of the sensors.

The sensitivity of this technique depends on the ratio of the major to minor axes of the ellipse defined by (1) and (2). The amplitude of the body tide as a function of azimuth is given by

$$A(\alpha) = k \sin(\theta)\left\{1 - \sin^2(\theta)\cos^2(\alpha)\right\}^{1/2} \qquad (3)$$

where k is a constant, θ is the colatitude of the station, and α is the azimuth of the sensor. The body tide ellipse is thus always oriented so that its major and minor axes are oriented east-west and north-south, respectively. The ratio of the axes of the ellipse depends on $\cos(\theta)$, so that ratios on the order of 1.5:1 are typical for stations in the United States. If the amplitude of M_2 can be measured to 1%, then this ellipticity implies that the azimuth can be determined with an uncertainty of about 1° using tidal data. The phase variation given by (2) yields a determination of the same order.

The actual ellipse at any station will be modified by the ocean load. This correction depends on the distance to the ocean and on other factors so that it cannot be easily estimated; it is of the order of 10% in the middle of the United States, but is significantly higher near the coast. If the ocean load is a strong function of the azimuth of the tiltmeter, its presence increases the usefulness of the measured tidal ellipse in determining the azimuth of an instrument.

Tilt Sensors

The tilt sensors are horizontal pendulums and the design is shown in Figure 3. A mass M is located at the end of a rigid beam B. The beam is supported by three wires, W_1, W_2, and W_3. Two important features of the mechanical design are the small springs (S) incorporated into each of the wires to protect the suspension from damage due to shock or vibration and the pantograph arrangement of the suspension which makes the period and the mechanical sensitivity independent of temperature to first order. The wires are attached to the frame of the instrument at P_1, P_2, and P_3, but the diameter and stiffness of each wire are chosen so that displacements of the mass are with respect to the virtual hinge points V_1, V_2, and V_3. These hinge points lie along a line offset from the vertical by a small angle i. If the vertical axis tilts out of the plane of the paper by a small angle d, the pendulum swings out

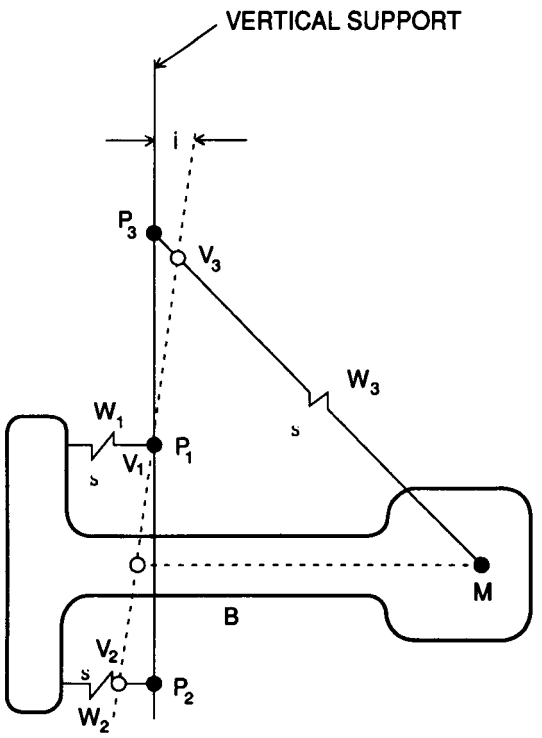

Fig. 3. A horizontal pendulum. A mass M is suspended at the end of a beam B using three wires W_1, W_2, and W_3. The wires are attached to the vertical support at points P_1, P_2, and P_3. The pendulum rotates about three virtual pivots V_1, V_2, and V_3 which lie along a straight line offset from the vertical by a small angle i. The small springs (S) protect the suspension from damage due to shock or vibration.

of the plane of the paper through an angle δ, where $\delta = d/i$. If the length of the beam is L, the mass moves a distance $L\delta = d(L/i)$. The time to reach the new equilibrium position is proportional to the period, which depends on $(L/i)^{1/2}$. In our instruments, $L \approx 10$ mm and $i \approx 2.3°$. The period is 1 s, the mass moves 0.24 μm/μrad, and the displacement of the pendulum in response to a tilt is equivalent to a vertical pendulum that is 240 mm long. The mechanical amplification (relative to a simple vertical pendulum of the same length as the beam) is thus about 24.

Each instrument consists of two pendulums mounted so that their sensitive axes are perpendicular to each other. The pendulums are mounted on a small plate as shown in Figure 4 and are protected from air currents and dust by a sealed cylindrical cover. The mounting arrangement isolates the pendulums from the flexing of the hermetically sealed case due to changes in barometric pressure. The case is approximately 65 mm high and 70 mm in diameter.

The base plate is supported on a three-point mount; two of the support points are motor-driven screws. These motors are used to level the instrument after the capsule is installed. The platform has a dynamic range of about 0.1 rad (5°), and the instruments can be zeroed to about 0.1 μrad. See Figure 5.

Each pendulum is suspended between two plates

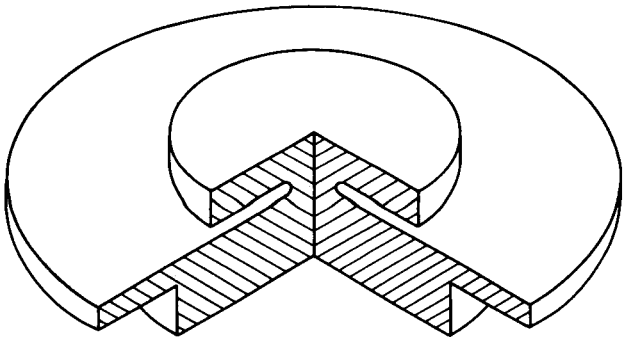

Fig. 4. Mounting plate. The pendulums are mounted on the raised inner plate so as to isolate them from the flexing of the base plate produced by atmospheric pressure changes acting on the sealed case.

separated by about 1 mm. The plates and the pendulum form two arms of a capacitance bridge; the other two arms are formed by the center-tapped secondary coil of a transformer. The primary of the transformer is driven by an ac signal and the amplitude and phase of the signal at the center plate are measured using a phase-sensitive detector. The gain of the circuit is adjusted to yield an overall sensitivity of approximately 2 V/μrad. The phase-sensitive detector and the amplifiers are located inside the capsule within a few centimeters of the pendulums.

The sensitivity of each pendulum is measured in our laboratory using a tilt table. Each pendulum is usually recalibrated whenever it is returned to Boulder. Successive calibrations agree to within 1% even if they are performed several years apart. Once the mechanical sensitivity of each pendulum has been determined, the gain of its amplifier is adjusted to yield the nominal overall sensitivity discussed above, and successive calibrations are then performed on the sensor-amplifier pair.

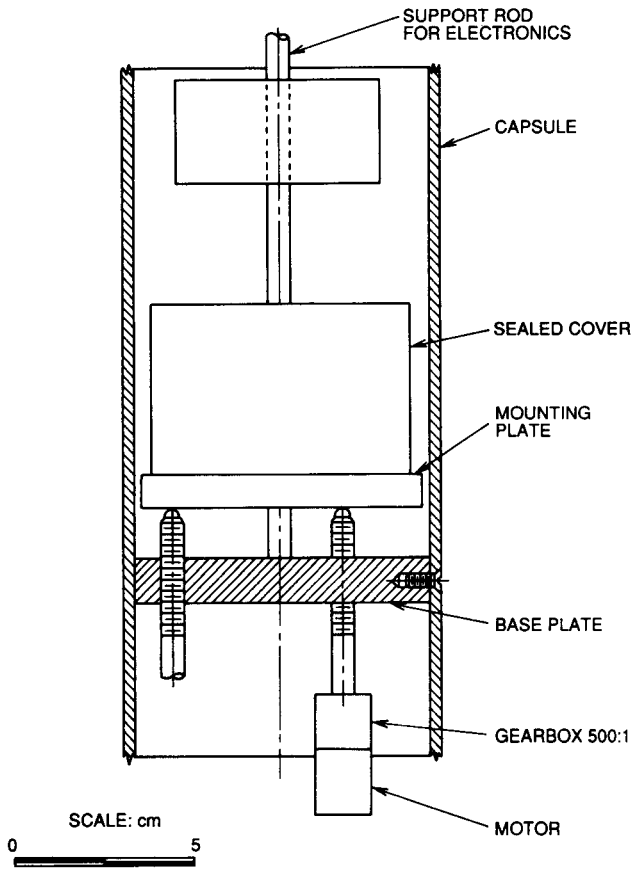

Fig. 5. The pendulums and the leveling system. The leveling screws have 4 threads/mm and are driven by small electric motors through 500:1 reducing gear boxes.

Filters and Digitizer

The outputs of the two phase-sensitive detectors are sent to the top of the borehole where they are low-pass filtered with a low-frequency gain of unity and using a time constant of 200 s. The voltages are then digitized; the least count of the digitizer is equivalent to a tilt of about 2 nrad and the digitizing frequency is 10 times per hour. The data are transmitted to our laboratory once per day using dial-up telephone lines. The details of the recording and transmission system are described by Levine [1985].

Power Supply

The entire tiltmeter system uses approximately 7 W. Most of this power is used by the digitizing and recording circuits. This power is provided by commercial power lines with battery backup. Great care is necessary to isolate the tiltmeter from the power line ground if fluctuations in ground currents are not to be a problem. Power line transients and large fluctuations in the input voltage are also a problem; these are quite common at remote sites and may be quite difficult to remove.

Preliminary Data Analysis

Almost all tilt records show significant secular signals, and these signals must be separated from the tides if unbiased estimates of the admittances are to be obtained. Simple situations may be dealt with using digital filters [Gold and Rader, 1969], but such filters are generally not optimum because the secular tilt has appreciable power at tidal periods. The tilt rate for a tidal component is about 1 nrad/h at a typical mid-latitude station. Borehole tiltmeters show long-term-average secular tilt rates only about 10 times less than this value (i.e., $\lesssim$ 1 μrad/yr) and secular rates of 1 nrad/h are quite often observed for several days at a time. Under these conditions the nontidal effects will have significant power in the tidal bands, and such tilts cannot be removed using frequency methods without at the same time either projecting significant tidal power into the secular tilt channel or biasing the tidal admittance with residual power from nontidal sources. In either case, the estimated tidal amplitude will depend on the instantaneous secular tilt rate.

Instead of digital filtering, we remove the

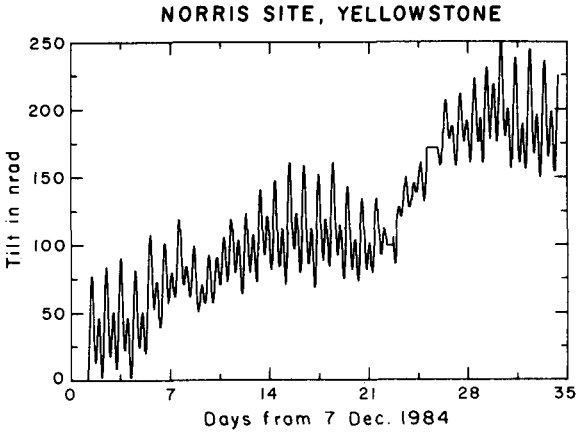

Fig. 6. Data recorded at Norris Geyser Basin in Yellowstone National Park.

secular drift in the time domain using cubic splines [Forsythe et al., 1977]. These are piecewise continuous cubic polynomials that pass through a series of points called knots [Ahlberg et al., 1967]. We choose the knots graphically using a digitizing table. If the secular tilt rate changes rapidly, conventional splines often oscillate and do not yield a monotonic secular tilt even though the knots are monotonic. In this case, we use the modified spline technique of Fritsch and Carlson [1979].

The advantage of the spline fit over digital filtering may be demonstrated using the data shown in Figure 6, which shows a tilt record obtained at Norris Geyser Basin in Yellowstone National Park. The record is typical of the data recorded at all of our sites except for the significantly larger secular tilts that are recorded when an instrument is first installed and during the spring thaw. Note that the secular and tidal tilt rates are often comparable.

We estimated the amplitudes and phases of the various tidal components using least squares as discussed below, and Figure 7 compares the spectra of the residuals with the power spectrum of the original data set when cubic splines or digital filters are used to remove the secular effects. The spline process is better able to cope with the vagaries of the baseline, and the residuals of the fit show a smooth background noise spectrum. (The small peak near 3 cycles per day is a terdiurnal tidal component that was purposely omitted from the fitting function.) The signal-to-noise ratio at 2 cycles per day is about 40 dB, and the formal uncertainty of the least squares determination of the tidal amplitude is 1.2%. The digital filter removes more low-frequency energy than the splines, and the power spectrum of the residuals computed using this method shows less energy at very low frequencies. The residual energy in the tidal band is almost 10 dB higher, however, and contains residual tidal energy because the digital filter is not efficient in estimating a process that is not well characterized in the frequency domain. The signal-to-noise ratio at 2 cycles per day is only about 22 dB, and the tidal amplitude estimate has a formal uncertainty of 6%. The two methods produce estimates of the amplitudes of the semidiurnal tides that disagree by 7%, which is roughly the sum of their formal uncertainties. Note that although the 3 cycles per day component is still present in the spectrum obtained from the filtered data, it cannot be resolved against the higher noise background.

Dealing with gaps in the data is also very important. We bridge the gaps by inserting estimates of the tides and the secular trend. The tides are estimated using the average admittance for the data set, while the secular trend is approximated using an appropriate straight line to make the time series continuous at the edges of the gap. The patching process is usually iterative: the insertion of a patch changes the average admittance of the data set, and this in turn implies a slightly different set of coefficients for the patch. When the process has converged, the residual tidal power in the patch is comparable to the incoherent power at tidal frequencies in the remainder of the data set. In this way, both the time and frequency domain representations of the patch are smooth across the tidal bands.

Estimating the Tidal Admittance

Although estimating the tidal admittance when the noise level is low is neither a new nor a particularly difficult problem, methods used for gravity data [Levine et al., 1986] must be modified to obtain robust estimates using tilt data because of the relatively poor signal-to-noise ratio of this type of measurement.

To estimate the tidal admittance, the tidal record at a station is compared with a parametrized version of the theoretical body tide. If a least squares procedure is used to fit the theoretical time series to the data, the fitting function is expanded either in spherical harmonics of the lunar and solar positions [Munk and Cartwright, 1966] or as a sum of frequencies [Cartwright and Tayler, 1971; Cartwright and Edden, 1973]. The first expansion converges much more rapidly than the Fourier series, and many

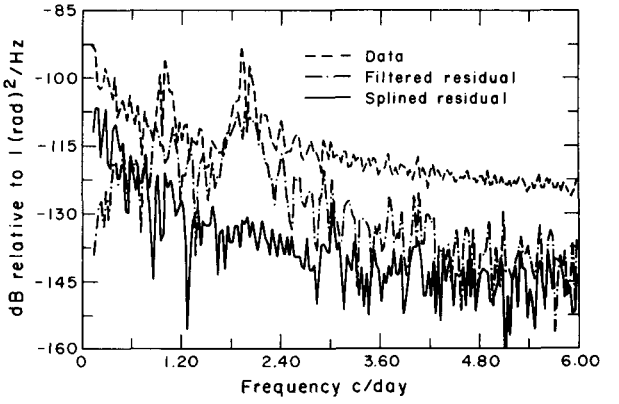

Fig. 7. Comparison of the spectrum of the data shown in Figure 6 with the spectrum of the residuals of a fit of the tidal potential when the secular tilt is removed using digital filters or splines. The peak near 3 cycles per day in the residuals of the spline process is a terdiurnal tidal component that was purposely left out of the fitting process.

fewer terms are required. It is easier to incorporate ocean loads and thermoelastic tilts into frequency expansions, however, since these effects are usually specified as functions of frequency. Alternatively, the Fourier transform of the data may be divided by the corresponding transform of a theoretical time series to yield the admittance directly.

If the amplitudes and phases of the components are estimated using ratios of Fourier transforms, then end effects, due to the finite length of the data set, must be considered. These end effects convolve the true spectrum with a "window" function [Blackman and Tukey, 1958]. Many different window functions exist; their goal is to reduce the admixture of frequencies removed from the frequency of interest (relative to what would be obtained using the default "boxcar" function), and they do so at the expense of resolution. That is, they do not attenuate (and may even increase) the influence of nearby frequencies. The effect of a particular window function may be calculated by convolving the transform of the window with the theoretical tidal spectrum from the tables of Cartwright and Edden [1973].

We have performed these convolutions for O_1 and M_2, the two components most often used in tidal analyses. If the amplitude of O_1 is estimated using a Fourier transform of a data set that is 1 month long, then a rectangular window will bias the estimate by 19% due to nearby lines (those within 2 cycles per year of O_1) and by 13% due to all other frequencies. If a Hamming or Hanning window is used [e.g., Schüller, 1977], the contribution due to the entire distant portion of the spectrum is reduced to less than 1%, while the contribution due to nearby frequencies is essentially unchanged. The calculation for M_2 is similar. The contribution due to the entire distant spectrum is reduced from 1% to a negligible value by choosing either window, but the contribution due to the nearby lines is about 4% and is essentially unchanged because the window function has a negligible effect on the nearby frequency components.

The influence of the distant portion of the spectrum decreases as the length of the data set increases, but the effect of the nearby lines is almost unaffected, even for data sets spanning a full year. If the site admittance is independent of frequency and if the incoherent power in the tidal bands is small, these end effects tend to cancel in the division of the two spectra, but this is not true for most of the tilt data sets we have obtained.

A least squares approach will yield unbiased estimates of the admittances of even closely spaced frequencies provided that the fitting potential contains enough degrees of freedom to adequately represent the data set (including estimates of nontidal effects such as local temperature and pressure). The variance of the estimates is primarily a function of the signal-to-noise ratio of the record [Munk and Hasselmann, 1964], and the difficulty in determining the amplitudes of closely spaced lines is that the variances of their estimates become too large to yield significant information. In practice, we combine nearby frequencies into groups and constrain the admittance within a group to be a constant value; the stability is improved at the expense of resolution.

The grouping of frequencies in this way has one important difference from the superficially analogous procedure of an expansion in spherical harmonics. We combine into one group frequencies that are close together even if they come from different spherical harmonics, whereas the spherical harmonic expansion would keep these terms separate. Thus the semidiurnal terms from Y_{32} are combined with the nearly degenerate terms from Y_{22} in the fitting process. The semidiurnal terms arising from Y_{32} have amplitudes that are roughly 2% of the Y_{22} contributions, since they are scaled by the lunar parallax. The frequencies of these terms may differ from the first-order tides by 1 cycle per year or less.

We use 14 groups in our least squares fits. Each group consists of all of the potential terms that differ from each other in frequency by less than about 1 cycle per month. There is one long-period group, seven nominally diurnal groups, five nominally semidiurnal groups, and one terdiurnal group. The maximum number of terms in any of the groups is 15, and all of the terms listed in the tidal table [Cartwright and Tayler, 1971; Cartwright and Edden, 1973] exceeding 0.1% of the potential are included. Each term in a group is multiplied by a coefficient which includes the Love numbers, the spherical harmonic of the station coordinates, and the angular factor to convert from tidal potential to tilt along the azimuth of the instrument. No explicit windowing of the data set is used. The coefficients of the fit are the tilt admittances, and the residuals provide an estimate of the nontidal power including the adequacy of the spline estimate of the secular tilt and the patches. If either the spline or the patches are deemed inadequate (because the residuals are significantly nonrandom either in long term or at a patch), the appropriate parameters are modified, and the analysis is repeated. The output of the process is a spline-smoothed secular tilt, a set of tidal admittances, and a residual time series.

Estimates of the tidal admittances should be normally distributed about the mean with a variance that can be estimated from the projection of the nontidal portion of the power spectrum of the data into the bandwidth of the analysis. This may not be true, but the results are inconclusive. It is unlikely that our results can be explained by cusps in the ocean load [Munk, et al., 1965; Cartwright and Amin, 1986], although an analogous site-specific nonlinearity is a possibility.

Tiltmeter Sites

We have installed tiltmeters at seven sites in Colorado and Wyoming. The locations of the stations are shown in Table 1.

The sites in Colorado were intended to test the instrument, to investigate the performance in boreholes of different depths, and to test the coherence among nearby instruments. The sites in Wyoming were all in Yellowstone National Park. The array was designed to investigate the spatial variation in the Earth tides in a region where the elastic parameters varied both horizontally and with depth. A comparison between the tidal results and a finite element model is presented by Meertens et al. [this issue].

TABLE 1. Locations of Tiltmeters

Name	Location	Coordinates	Depths, m
NBS	Boulder, Colorado	39.993°N,105.269°W	15, 30
ERE	Erie, Colorado	40.095°N,105.045°W	30, 30
TWR	Tower Junction, Yellowstone	44.925°N,110.425°W	30, 30
CAN	Canyon Village, Yellowstone	44.738°N,110.498°W	30, 30
MAD	Madison, Junction, Yellowstone	44.652°N,110.840°W	30, 30
LAK	Yellowstone Lake	44.559°N,110.401°W	30, 30
NOR	Norris Geysers, Yellowstone	44.740°N,110.692°W	30, 30

Results and Discussion

Boulder, Colorado, Site

The site in Boulder (NBS) is located near the boundary between the Precambrian igneous and metamorphic rocks to the west and the Phanerozoic sediments to the east. The boreholes are located on a hillside; the secular tilt rate varied from less than 0.1 to almost 1 μrad/yr. The boreholes are of different depth, and the shallower boreholes show significant tilts correlated with rainfall and the seasons as discussed above. The deeper boreholes do not show these effects, and the correlation among the long-period tilt records is therefore small.

In Figure 8 we show the power spectrum of a tilt record obtained at the NBS site using a horizontal pendulum in a 30-m borehole. The record was 1 month long and was processed according to the methods described above. The signal-to-noise ratio in the semidiurnal band, measured by comparing the signal power to the residual power is about 35 dB or about 50:1 in amplitude. The uncertainty in the admittances should then be of the order of 2%. The signal-to-noise ratio in the diurnal band is only 20 dB because of the sensitivity of the site to the diurnal pressure and temperature fluctuations acting both directly on the instrument and indirectly through thermoelastic effects. The uncertainty in the diurnal admittance should then be about 10%.

Table 2 shows the results of consecutive monthly estimates of the admittance using the horizontal pendulums in the 30-m borehole. The data from the two pendulums are combined to yield tilts along the north-south and east-west directions, and the amplitudes and phases of the tides are then estimated with respect to the body tides. The azimuthally averaged M_2 amplitude is 0.993 ± 0.04 and the average phase is -4.54° ± 2.3°, where a negative sign implies a phase lead. The difference between measurements on different azimuths is not significant. The results for O_1, however, depend on the azimuth of the instrument. The admittance along an azimuth of 90° is 1.2 with a phase of 4.5°; the corresponding values

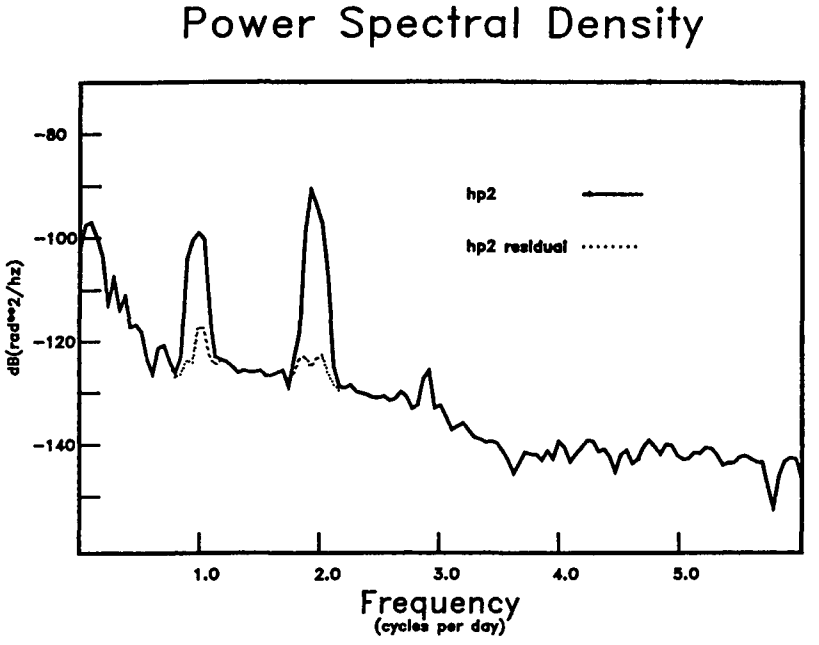

Fig. 8. The power spectrum of a data set 28 days long. The data were recorded using a pair of horizontal pendulums in a 30-m borehole in Boulder, Colorado. The dotted curve shows the residuals of a fit to remove the diurnal and semidiurnal tides. The long-period and terdiurnal tides were not removed, and the two spectra are therefore identical at these frequencies.

TABLE 2. Admittance at NBS Site for Consecutive 28-day Averages

Period	M_2 (1.9323 cycles per day)				O_1 (0.9295 cycles per day)			
	Amplitude		Phase, deg		Amplitude		Phase, deg	
	N-S	E-W	N-S	E-W	N-S	E-W	N-S	E-W
Oct. 1980	1.06	1.02	-0.49	-0.77	0.80	1.11	-7.7	0.0
Nov. 1980	0.92	0.94	-7.60	-3.30	0.84	1.22	-8.7	8.8
Dec. 1980	1.01	0.99	-3.90	-5.90	0.93	1.30	-1.4	6.3
Jan. 1981	0.94	0.99	-4.50	-4.30	0.96	1.31	-0.9	10.0
Feb. 1981	1.03	1.04	-6.40	-6.35	0.96	1.08	-6.4	0.8
March 1981	1.01	1.05	-3.10	-2.20	0.87	1.15	-0.0	3.5
April 1981	0.92	0.97	-7.50	-7.80	0.82	1.15	-9.3	4.1
May 1981	0.99	1.01	-4.50	-4.10	0.96	1.30	-5.6	2.2
Average	0.985	1.00	-4.75	-4.34	0.89	1.20	-5.0	4.5
Standard Deviation	±0.05	±0.04	±2.4	±2.3	±0.07	±0.09	±3.7	±3.7
Theory Body + Load + Topography	0.96	0.975	-6.00	-6.00	0.83	1.20	-15.0	5.0

The amplitude and phase are with respect to the body tilt along the specified axis. A negative phase is a lead.

for the north-south direction are 0.89 and -5°. The standard deviations of consecutive monthly estimates are ±8% in amplitude and ±4° in phase.

These results may be evaluated by adding the effects of ocean loading and topography to the body tide. D. Agnew performed the ocean load calculations for us using Goad's [1980] integrated Green's function algorithm and T. Sasao used Farrell's [1972, 1973] technique. The two calculations yield essentially identical results.

The sum of the M_2 tide and load vectors has an amplitude of 0.96 with respect to the body tide and a phase lead of -6°, and these values are independent of azimuth. The phase relationship between the ocean load and the body tide for O_1 depends significantly on azimuth; the admittances with respect to the body tide are 0.83 and -15° along the north-south direction and 1.20 and 5° along east-west.

The correction for topography follows the almost identical calculation of Levine and Harrison [1976]. The contribution at M_2 increases the tidal amplitude by 1.5% in the east-west direction and has a negligible effect along the perpendicular azimuth. The result is an admittance with an azimuthal dependence, but the effect is too small to be resolved in our data. The topographic contribution to the O_1 estimate is not significant.

The agreement between experiment and theory is consistent with the uncertainty estimate based on the power spectrum of Figure 8 and the formal error of the mean of the consecutive monthly values. There is also no evidence for time dependence in either admittance.

Erie, Colorado, Site

Erie is about 25 km east of Boulder in a region characterized by thick sediments and flat topography. The site was chosen to provide a contrast with our Boulder site. The boreholes are 30 m apart and 30 m deep. The tiltmeters in the two boreholes have independent electronics and power supplies, although the data are recorded and transmitted to Boulder via a common system.

The background noise at the site was approximately 6-8 dB higher than we measured at Boulder, perhaps because of the difference in the material properties. The secular tilt rate was quite variable and ranged from 0.2 to 1.0 μrad/yr. Tilt rates up to 5 μrad/yr were observed for periods of up to a month.

Figures 9 and 10 compare the nontidal tilts measured in two boreholes at Erie. The nontidal tilt is the sum of the spline estimate of the baseline, which is used to model signals with

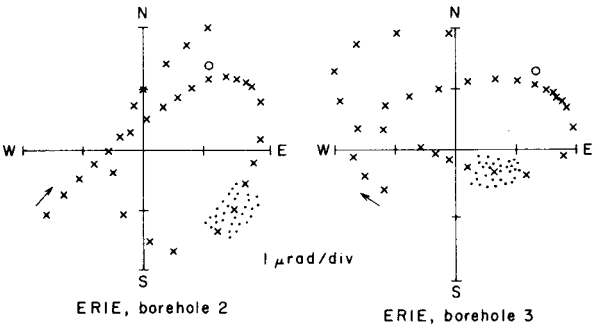

Fig. 9. A comparison of the long-period tilt recorded by two instruments at Erie. The points are traversed in the direction shown by the arrow. Each cross represents a 1-month average composed of daily estimates, a representative set of which are shown by dots. The first point is for April 1981. The circle shows the location of the data plotted in Figure 10.

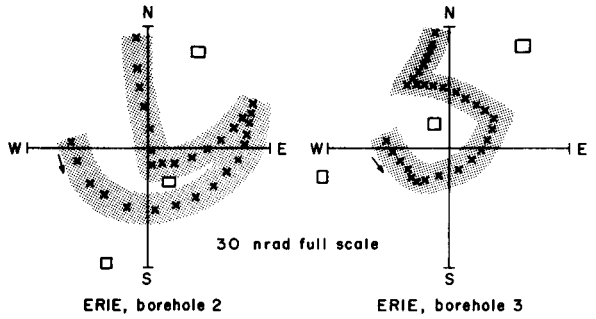

Fig. 10. Tidal residuals from two tiltmeters at Erie starting at 0 hours on February 1, 1982 (shown by a circle in Figure 9). Consecutive 6-min estimates fall within the shaded region, and hourly averages are plotted with an cross. The points are traversed in the direction shown by the arrow.

periods of a few days and longer, and the residuals of the fit of the tidal potential, which are used to estimate the shorter-period effects. Each plot shows the vector sum of the nontidal signals recorded by the two sensors in the borehole (relative to an arbitrary origin). The secular tilts recorded for 30 months beginning in April 1981 are shown in Figure 9. Monthly averages are plotted as crosses, and 30 daily estimates, computed from data sets like the one shown in Figure 10, are shown by dots. Both tiltmeters record a tilt to the north-east at an average rate of 1.0-1.2 μrad/yr and both show a 2-year periodicity with a similar amplitude, although the phase is not the same in the two boreholes.

Figure 10 shows a small segment (shown by a circle in Figure 9) of the same data. The residuals are computed every 6 min and are then averaged and decimated to one value per hour. The hourly values are plotted as crosses in Figure 10. The 6-min points that make up the first 12 averages are shown by dots. The daily average is shown by a square; the averages for the two adjacent days are also shown.

We have computed the coherence between the two tiltmeters as a function of frequency using the hourly tidal residuals. Each data set is divided into thirty 28-day blocks, the Fourier transform of each block is computed with no explicit window function, and the coherence at each frequency is computed as the average cross spectrum divided by the average power. The result is shown in Figure 11. The estimates have 30 degrees of freedom, and the difference between the estimated and true coherences is less than 0.22 at the 95% confidence level [Haubrich, 1965]. We find significant coherence for frequencies ranging from 0.5 to 2 cycles per day even after the tides have been removed. The coherence decreases to a much lower value at both higher and lower frequencies.

Based on the increased noise level compared to Boulder, we would have expected an increase in the uncertainties of the admittance estimates by a factor of 2, but a larger increase was in fact found. The standard deviation of consecutive monthly estimates was 15%, a factor of 3 larger, with some evidence that the admittance was a function of the low-frequency noise. Figure 12 shows monthly M_2 admittances as a function of the average power in the data set at periods of 7 days or longer, while Figure 13 shows the same admittances as a function of the power at 1.5 cycles per day (well away from the tides). When plotted as a function of residual power at 1.5 cycles per day, the admittance is independent of the residual power at a confidence level of 75%. The mean (1.06) and standard deviation (±15%) are shown by the dashed curves. The admittance is correlated with the low-frequency power, however, with a coefficient of 0.02 dB^{-1}. The standard deviation of this estimate is 0.012 so that the dependence of the admittance on low-frequency power is nonzero at the 70% confidence level. We cannot explain this interaction between the tides and the long-period noise.

Yellowstone National Park Sites

The Yellowstone array was designed to test the hypothesis that the tides would be significantly

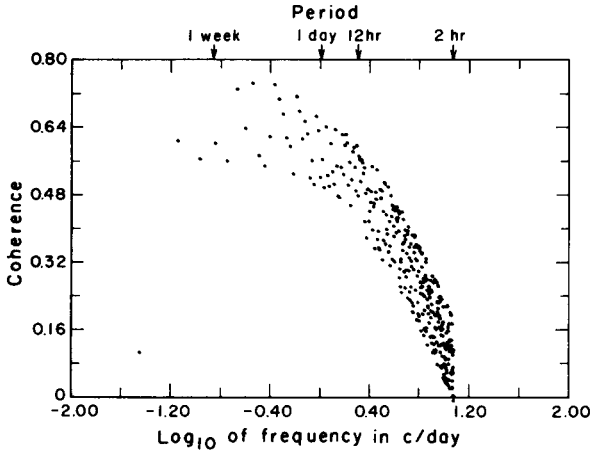

Fig. 11. Coherence between two tiltmeters at Erie, Colorado, as a function of frequency.

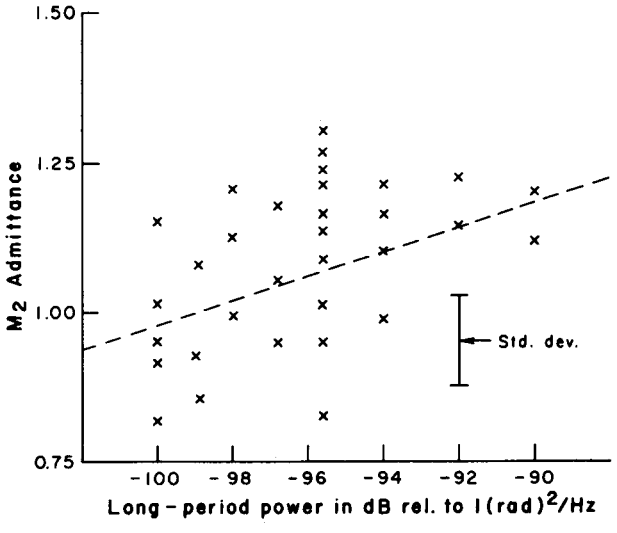

Fig. 12. M_2 admittance at Erie, Colorado, as a function of the low-frequency noise power. The ordinate is in units of the body tide along the azimuth of the tiltmeter. The dashed curve is a least squares fit to the points.

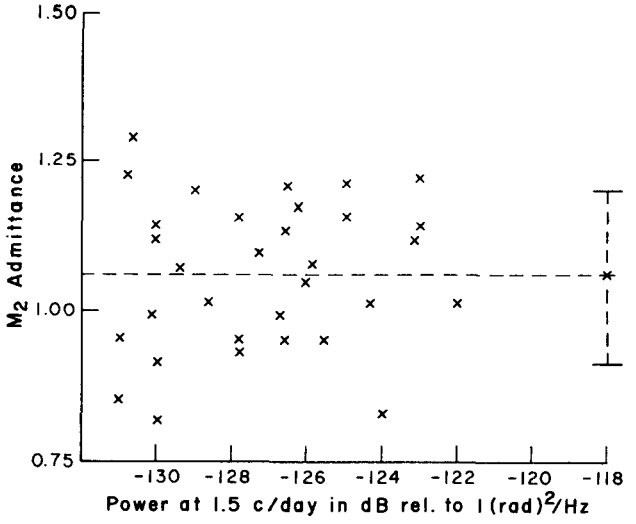

Fig. 13. M_2 admittance at Erie, Colorado, as a function of the power at 1.5 cycles per day. The ordinate is in units of the body tide along the azimuth of the tiltmeter. The dashed curve is a least squares fit to the points.

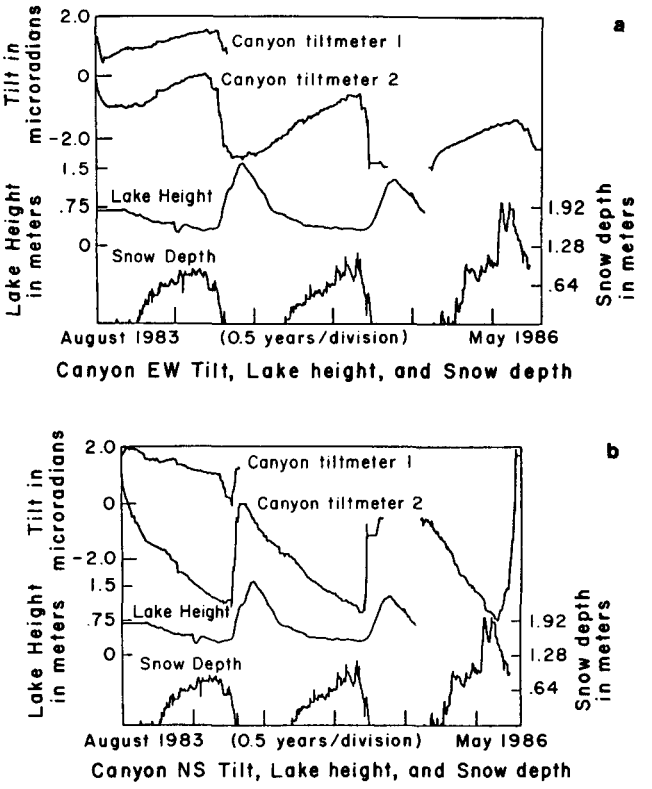

Fig. 14. Secular tilt at Canyon compared with the height of Yellowstone Lake and approximate snow depth. The large tilt in the spring of each year is apparently related to the change in the level of the lake and the changes in the water table that accompany the melting of the large snow pack. The Lake height data and the snow depth were provided by W. Hamilton of the National Park Service. (a) East-west component. (b) North-south component.

modified near the boundary between two regions of different elastic properties [Beaumont and Berger, 1974]. The sites were therefore chosen near the edges of the anomalous, partially molten body as defined by Eaton et al. [1975], Smith et al. [1982], and others. The need for telephone and power lines and the requirements of the National Park Service constrained the sites to be in service areas.

Two holes, a few meters apart, were drilled at each of five sites (Table 1). The nominal depth of each hole was 30 m, although the actual depths varied somewhat due to local conditions. The bottom of the borehole was below the water table at all sites. All of the boreholes were not in use simultaneously, since we did not have 10 tiltmeters, but simultaneous records from both boreholes were recorded at Canyon and Lake.

All of the tiltmeters used in the Yellowstone experiment were first operated in Colorado for several months to evaluate their performance, and each instrument was calibrated whenever it was returned to Boulder. The calibration factor of each instrument was stable to 1%.

The secular tilt rate at all of the sites varied from 0.5 to 1.0 μrad/yr. In addition, there are large annual (and 24-month period) tilts that are correlated with changes in the water table and the snow level (Figure 14). The annual cycle is asymmetric, showing a gradual accumulation during the fall and winter followed by a rapid decrease in the spring. The east-west component of the annual cycle is a regional effect; tiltmeters at Madison and Lake (about 35 km apart) show the same annual cycle, even though the tilts at shorter periods are quite different (Figure 15). There is more variability in the north-south component (Figure 16), and western stations, such as Madison, showed a much smaller decrease in the spring of 1985, followed by a larger, compensating decrease in 1986.

We searched for, but could not find, correlations between the secular tilt and local effects such as radon emission and variations in hydrothermal activity.

A detailed discussion of the Earth tide measurements and a comparison with the predic-

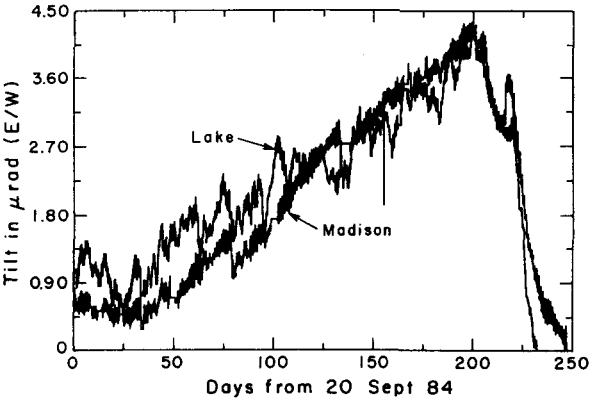

Fig. 15. Comparison of the east-west tilt at Lake and Madison.

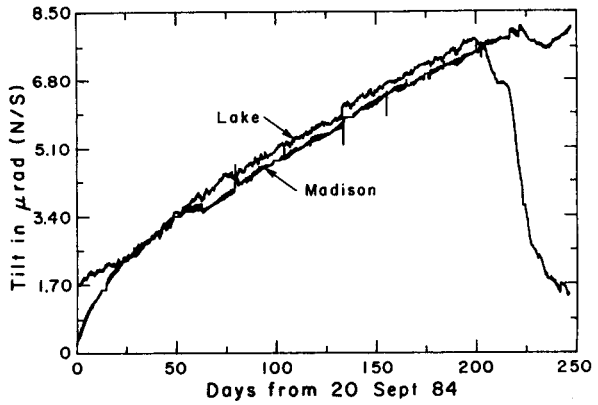

Fig. 16. Comparison of the north-south tilt at Lake and Madison.

tions of a finite element model of the region are given by Meertens et al. [this issue].

Conclusions

We have designed a borehole tiltmeter and associated hardware and software, and we have used the system to study secular and tidal tilt in Colorado and Yellowstone National Park, Wyoming. The tiltmeters have a dynamic range of 5 μrad and a resolution of 2 nrad. The instrumental response is linear to within 0.3%.

We measured secular tilt rates that varied from 0.5-1.0 μrad/yr, with the Yellowstone instruments showing larger annual signals that are correlated with changes in snow pack and groundwater level. There is significant coherence between tilts at intermediate periods measured by closely spaced instruments, but long-period tilts (except for the annual cycle in Yellowstone) show much less correlation.

We have found good agreement between measurements of the Earth tides in Colorado and values to be expected based on simple, first-order models; monthly estimates typically show formal errors of the order of 2%, but consecutive, nominally identical estimates deviate by more than this value from the mean. Our data from Erie suggest a coupling between the tides and the noise at longer periods. We cannot explain these observations.

Acknowledgments. We gratefully acknowledge the support of the Air Force Geophysics Laboratory under contracts F-19628-78-C-0065 and F-19628-81-K-0040. We are also very grateful to the Superintendent of Yellowstone, to Wayne Hamilton, the scientific coordinator, and to the many area rangers who allowed us to work in the park and were very helpful in many ways. Chris Harrison, formerly of the Department of Geological Sciences of the University of Colorado, also worked on the initial stages of the project and provided useful advice throughout the work. J. L. is a staff member of the NBS Time and Frequency Division.

References

Ahlberg, H. J., E. N. Nilson, and J. L. Walsh, The Theory of Splines and Their Application, Academic, San Diego, Calif., 1967.

Beaumont, C., and J. Berger, Earthquake prediction: Modification of the Earth tides and strains by dilatancy, Geophys. J. R. Astron. Soc., 39, 111-121, 1974.

Blackman, R. B., and J. W. Tukey, The Measurement of Power Spectra, p. 11 ff., Dover, New York, 1958.

Bonatz, M., C. Gerstenecker, R. Kistermann, and J. Zschau, Tilt measurements across a deep fault zone, in Proceedings of the Ninth International Symposium on Earth Tides, New York, pp. 695-702, Schweitzerbart'sche Buchhandlung, Stuttgart, 1983.

Cartwright, D. E., and M. Amin, The variances of tidal harmonics, Dtsch. Hydrogr. Z., 39, 235-253, 1986.

Cartwright, D. E., and A. C. Edden, Corrected tables of tidal harmonics, Geophys. J. R. Astron. Soc., 33, 253-264, 1973.

Cartwright, D. E., and R. J. Tayler, New computations of the tide-generating potential, Geophys. J. R. Astron. Soc., 23, 45-74, 1971.

Eaton, G. P., R. L. Christiansen, H. M. Iyer, A. M. Pitt, D. R. Mabey, H. R. Blank, Jr., I. Ziety, and M. E. Gettings, Magma beneath Yellowstone National Park, Science, 188, 787-796, 1975.

Farrell, W. E., Deformation of the Earth by surface loads, Rev. Geophys., 10, 761-797, 1972.

Farrell, W. E., Earth tides, ocean tides and tidal loading, Philos. Trans. R. Soc. London, Ser. A, 274, 253-259, 1973.

Forsythe, G. E., M. A. Malcolm, and C. B. Moler, Computer Methods for Mathematical Computations, p. 70 ff., Prentice-Hall, Englewood Cliffs, N. J., 1977.

Fritsch, F. N., and R. E. Carlson, Monotone piecewise cubic interpolation, Rep. UCRL-82453, Lawrence Livermore Lab., Livermore, Calif., 1979.

Gerstenecker, C., J. Zschau, and M. Bonatz, Finite element modelling of the Hunsrück tilt anomalies--A model comparison, in Proceedings of the Tenth International Symposium on Earth Tides, Madrid, pp. 797-804, Consejo Superior de Investigaciones Cientificas, Madrid, 1985.

Goad, C. C., Gravimetric tidal loading computed from integrated Green's functions, J. Geophys. Res., 85, 2679-2683, 1980.

Gold, B., and C. M. Rader, Digital Processing of Signals, McGraw-Hill, New York, 1969.

Harrison, J. C., Cavity and topographic effects in tilt and strain measurements, J. Geophys. Res., 81, 319-328, 1976.

Haubrich, R. A., Earth noise, 5 to 500 millicycles per second, J. Geophys. Res., 70, 1415-1427, 1965.

Levine, J., A study of secular and tidal tilt in Wyoming, Rep. AFGL-TR-86-0212, Air Force Geophys. Lab., pp. 30 ff., Hanscom Air Force Base, Mass., 1985.

Levine, J., and J. C. Harrison, Earth tide measurements in the Poorman Mine near Boulder, Colorado, J. Geophys. Res., 81, 2543-2555, 1976.

Levine, J., J. C. Harrison, and W. Dewhurst, Gravity tide measurements with a feedback gravity meter, J. Geophys. Res., 91, 12,835-12,841, 1986.

Meertens, C., J. Levine, and R. Busby, Tilt observations using borehole tiltmeters, 2. Analysis of data from Yellowstone National Park, J. Geophys. Res., this issue.

Munk, W. H., and D. C. Cartwright, Tidal spectroscopy and prediction, Proc. R. Soc. London, Ser. A, 259, 533-581, 1966.

Munk, W., and K. Hasselmann, Super-resolution of the tides, in Studies in Oceanography, pp. 339-344, Tokyo, 1964.

Munk, W., B. Zetler, and G. W. Groves, Tidal cusps, Geophys. J. R. Astron. Soc., 10, 211-219, 1965.

Schüller, K., Standard tidal analysis and its modification by frequency domain convolution, in Proceedings of the 8th International Symposium on Earth Tides, Bonn, pp. 94-102, Institut für Theoretische Geodäsie der Universität Bonn, 1977.

Smith, R. B., L. W. Braile, M. M. Schilly, J. Ansorge, C. Prodehl, M. Baker, J. H. Healy, S. Mueller, and R. Greenfelder, The 1978 Yellowstone-eastern Snake River Plain seismic profiling experiment: Crustal structure of the Yellowstone region and experiment design, J. Geophys. Res., 87, 2583-2596, 1982.

Wyatt, F., and J. Berger, Investigations of tilt measurements using shallow borehole tiltmeters, J. Geophys. Res., 85, 4351-4362, 1980.

Wyatt, F., G. Cabaniss, and D. C. Agnew, A comparison of tiltmeters at tidal frequencies, Geophys. Res. Lett., 9, 743-746, 1982.

R. Busby, Lamont-Doherty Geological Observatory, Seismology Bldg., Palisades, NY 10964.

J. Levine, Joint Institute for Laboratory Astrophysics, University of Colorado, Boulder, CO 80309-0440.

C. Meertens, Department of Geology and Geophysics, 615 W. Browning Bldg., University of Utah, Salt Lake City, UT 84112.

(Received September 22, 1987;
revised August 29, 1988;
accepted August 31, 1988.)